

Polyol Synthesis of Ruthenium Selenide Catalysts for Oxygen Reduction Reaction[†]

Ki Rak Lee and Seong Ihl Woo*

Department of Chemical and Biomolecular Engineering (BK21 Graduate Program),
Korea Advanced Institute of Science and Technology, Daejeon 305-701, Korea. *E-mail: siwoo@kaist.ac.kr
Received July 14, 2010, Accepted September 30, 2010

Ruthenium catalysts modified by selenium have been introduced as alternative materials to Pt in Direct methanol fuel cells (DMFCs). RuSe nano-particles were synthesized on the Vulcan XC72R carbon supports *via* polyol method. The prepared catalysts were electrochemically and physically characterized by cyclic voltammetry (CV,) linear sweep voltammetry, methanol tolerance test, X-ray diffraction (XRD), Transmission electron microscopy (TEM), Energy-dispersive Spectrometer (EDS) and X-ray photoelectron spectroscopy (XPS). Increasing the Se concentration up to 20 at % increased the electro-catalytic activity for the oxygen reduction. By increasing Se amount, Ru metallic form on the surface was increased. The Ru₈₀Se₂₀/C catalysts showed the highest oxygen reduction reaction (ORR) activity and outstanding methanol tolerant property in half cell tests as well as single cell test.

Key Words: Ruthenium-chalcogenide, Fuel cell, Oxygen reduction reaction, Electro-catalysts, Methanol tolerant property

Introduction

DMFCs are becoming promising power sources to substitute fuel combustion energies as well as batteries in portable electronic devices.¹⁻⁵ Significant and intensive investigations in this field have been progressed to commercialize this device. Until now, all low-temperature fuel cells including DMFCs have used platinum or platinum based materials as the electrode. PtRu alloy catalysts are widely used as the anode material.^{6,7} In the cathode, platinum shows an outstanding performance for oxygen reduction such as the highest catalytic activity and stability. Its high cost, however, is a serious problem. This problem has to be solved for successful commercialization. To solve the economic problem, Pt-transition metal alloy materials such as PtNi,^{8,9} PtCo,^{10,11} and PtCr¹² are developed as ORR catalysts. Furthermore, ternary or quaternary Pt based catalysts^{13,14} and Pt nano-particles with new support materials¹⁵⁻¹⁷ are introduced. These materials show the improved ORR activity because prevention of the particle sintering, surface roughening from the removal of some alloy metal, proper crystallographic geometry, and change of Pt-Pt inter-atomic distance causing change of Pt electro binding energy.^{18,19} Amounts of platinum, however, are still needed and it is not enough. Furthermore, platinum based catalysts show low methanol tolerance property. It is not suitable for the cathode material in DMFCs. Amount of methanol crossover generally occurs from the anode to cathode in DMFCs. Methanol crossover is the main reason for the drop in performance in the cathode.^{20,21} Development of economic catalysts with high ORR activity and methanol tolerant property is needed.

Recently, many researchers have interested in the development of Pt-free materials for oxygen electro-reduction. Efforts have been made to develop the non-platinum ORR catalysts such as Pd alloy materials,²²⁻²⁴ transition-metal macrocyclic compounds,^{25,26} Ru based materials,^{14,27,28} and N doped carbon

materials.²⁹⁻³¹ The approach of non-Pt catalysts not only makes fuel cells economical but also clears methanol crossover problem. Among various non-Pt catalysts, Ru based catalysts show good catalytic activity in ORR and high selectivity for four-electron reduction of oxygen to water in acidic media. The Ru based chalcogenides can be divided into Chevrel phases³² and amorphous ruthenium chalcogenides.³³ The former shows good performance as a cathode material. They are generally prepared by solid-state reaction in high temperature and pressure which is very complicated and expensive. The latter shows efficient activity for ORR in acidic media at low temperatures.

In this study, the Ru-chalcogenide (RuSe) nano-particles were synthesized on the carbon support *via* polyol method and an optimum composition was found. Polyol reduction is a well known process for synthesizing metallic nanoparticles.³⁴ For comparison, Ru/C was prepared with the same process. The prepared RuSe/C catalysts were tested for electro-chemical studies in half-cells as well as in single cells, and physical characterizations were carried out by XRD and XPS.

Experimental

RuSe nano particles were deposited on Vulcan XC72R using ethylene glycol as a reducing agent *via* polyol process.³⁵ Ruthenium acetylacetone and selenium tetrachloride were dissolved in ethylene glycol and then Vulcan XC72R was added to the solution. The suspension was sonicated and stirred for 1 h under N₂ condition. The suspension was then refluxed at 160 °C under N₂ condition with continuous stirring for 4 h. After the reflux, the suspension was filtered and washed with DI water and ethanol. Finally, the catalysts were dried at 80 °C, overnight. The prepared catalysts are denoted as Ru/C, Ru₉₅Se₅/C, Ru₉₀Se₁₀/C, Ru₈₅Se₁₅/C, Ru₈₀Se₂₀/C, and Ru₇₅Se₂₅/C to their atomic composition ratios. The Ru_xSe_{100-x}/C notation means a prepared ratio. Loading of metals was 60 wt %. All chemicals were analytical grade or better and were purchased from Sigma-Aldrich.

*This paper is dedicated to Professor Hasuck Kim for his outstanding contribution to electrochemistry and analytical chemistry.

XRD analysis was performed using a Cu K α radiation with a D/MAX-IIIC diffractometer for characterization of structural properties of the powder catalysts. XPS measurements were performed using Al K α radiation and the constant pass energy of 25 eV. The XPS peak software version 4.1 was used, and spectral peaks were fitted using a mixed Gaussian-Lorentzian (80:20) line and Shirley baselines. TEM analysis was done on a field emission transmission electron microscope (Tecnai G² F30 S-Twin). EDS analysis was carried out using a field emission SEM (Nova230) at an acceleration voltage of 20 kV.

Electrochemical analysis was carried out in a three electrode cell with a platinum counter electrode, an Ag/AgCl reference electrode (BAS Co., Ltd., MF-2052 RE5B), and a glassy carbon working electrode (3 mm dia, BAS Co., Ltd., MF-2012). The working electrodes were prepared by the thin-film electrode method³⁶ and had a loading of 80 μ g catalyst. The prepared electrodes were tested for CV and linear sweep voltammetry tests. The CV test was performed between 0.0 and 0.8 V (vs. reference hydrogen electrode (RHE)) at a scan rate of 15 mV s⁻¹. Nitrogen purged 1 M HClO₄ solution was used as an electrolyte. The linear sweep voltammetry was performed by rotating the working electrodes at a scan rate of 5 mV s⁻¹ in oxygen saturated 1 M HClO₄ solution and in oxygen saturated 1 M HClO₄ + 0.1 M methanol solution, respectively. All electrochemical experiments were carried out at room temperature and at ambient pressure. All potentials in this study were converted to RHE scale.

The membrane electrode assemblies (MEAs) were fabricated by spraying the catalyst onto Nafion 112. The anode catalyst was PtRu/C (E-tek, 60 wt %, Pt:Ru = 1:1 atomic ratio) and the cathode catalyst was Pt/C (E-tek, 60 wt %) and Ru₈₀Se₂₀/C. The catalyst loading was 2.5 mg cm⁻². The catalyst-coated membranes were hot-pressed at 120 °C for 3 min. Polarization curves were obtained using a homemade single cell with an active area of 4 cm². 1 M methanol and oxygen were fed into the anode and cathode at the flow rate of 1 mL min⁻¹ and 100 cc min⁻¹, respectively. The single cells were operated at 70 °C.

Results and Discussions

Fig. 1(a) shows a TEM image of the Ru₈₀Se₂₀/C catalyst. There are nano sized metal particles on the carbon support. However, a non-homogeneous particle distribution is observed due to the high RuSe loading. Reliable analysis of the particle size is difficult from TEM image. The particle size of each catalysts was calculated from XRD analysis. XRD results of the synthesized catalysts are shown in Fig. 1(b). The broad peak at 20 value of 25° was related to (002) plane of the hexagonal structure of Vulcan XC-72R carbon support.³⁷ Selenium or selenide phase was not detected in XRD results. It is the reason that the selenium is present in the form of a fully amorphous phase or the amount of crystalline selenium is below the XRD sensitivity.³⁸ The (110) diffraction peak of crystallographic Ru plane was used for analysis of the structural properties. The (110) peaks were observed at 20 values of 69.40° for Ru/C, 69.40° for Ru₉₅Se₅/C, 69.42° for Ru₉₀Se₁₀/C, 69.45° for Ru₈₅Se₁₅/C, 69.50° for Ru₈₀Se₂₀/C, and 69.50° for Ru₇₅Se₂₅/C, respectively. The (110) peaks of the synthesized catalysts appear-

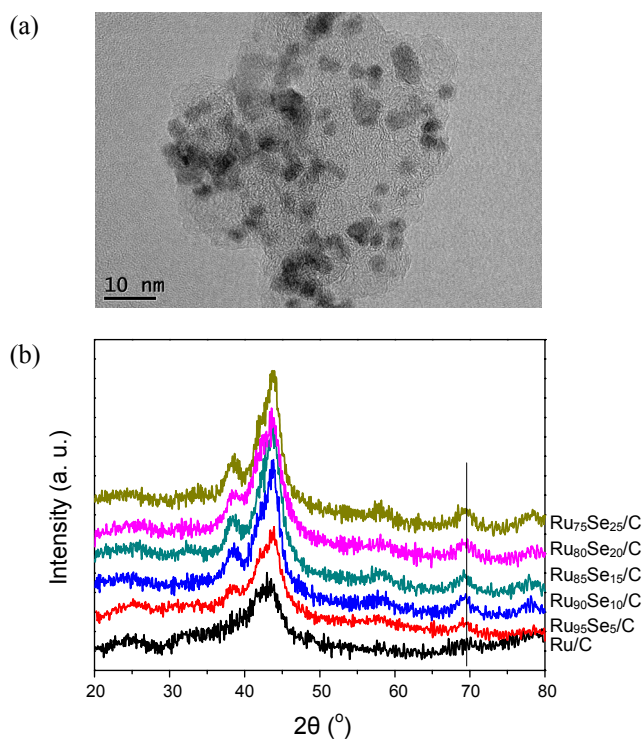


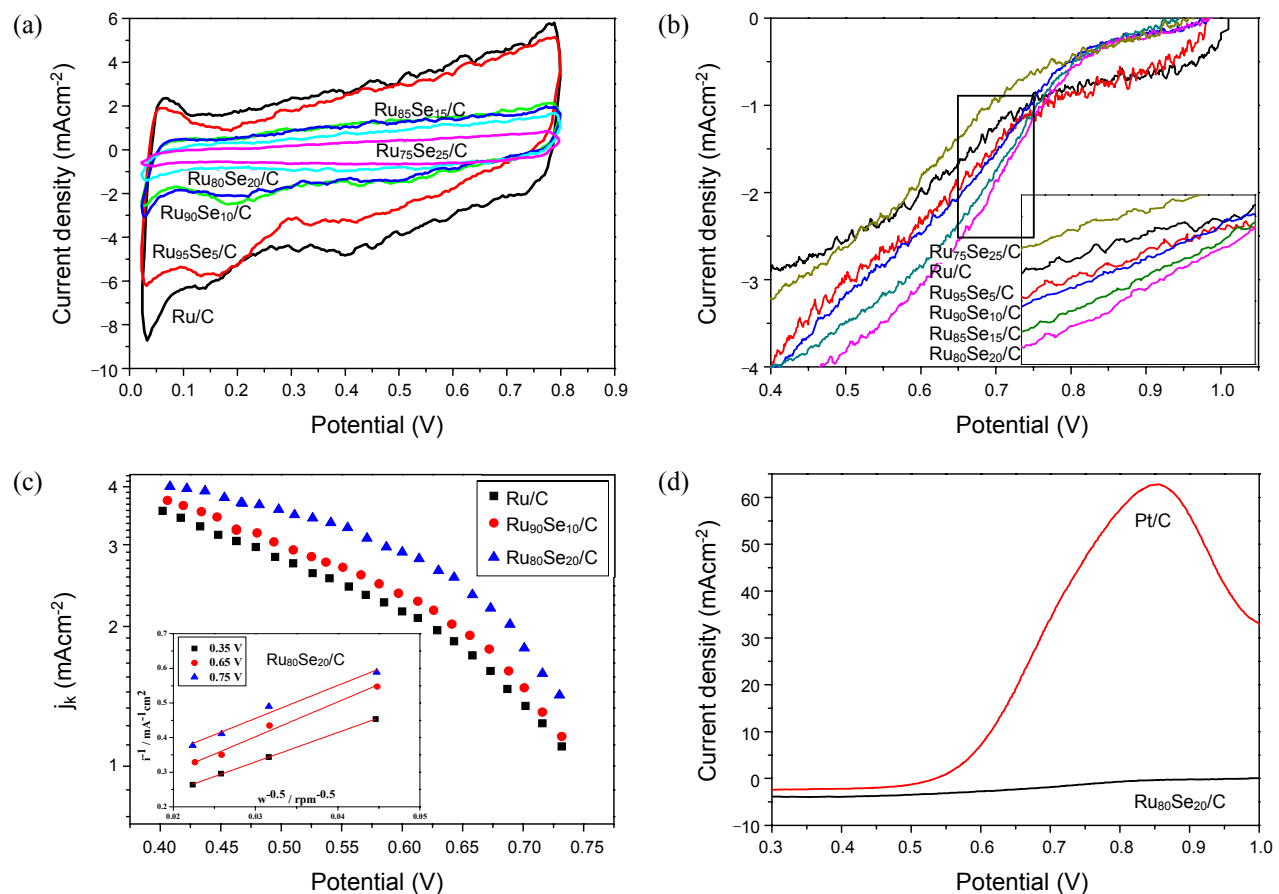
Figure 1. TEM image of the Ru₈₀Se₂₀/C catalyst (a) and XRD results of the Ru/C, Ru₉₅Se₅/C, Ru₉₀Se₁₀/C, Ru₈₅Se₁₅/C, Ru₈₀Se₂₀/C, and Ru₇₅Se₂₅/C catalysts (b).

ared at similar 20 values, indicating the low degree of alloy in most catalysts. The average particle sizes were calculated using the Debye-Scherrer equation.³⁹ Average particle sizes were 4.9, 5.1, 3.9, 3.6, 4.1, and 4.6 nm for the Ru/C, Ru₉₅Se₅/C, Ru₉₀Se₁₀/C, Ru₈₅Se₁₅/C, Ru₈₀Se₂₀/C, and Ru₇₅Se₂₅/C, respectively. The EDS data showed the purposed bulk compositions of Ru and Se on each catalyst. However, selenium was not detected from XRD analysis. It means that the Se forms an amorphous phase on the RuSe catalysts. A summary of the XRD and EDS results are listed in Table 1.

Electrochemical analysis of the synthesized catalysts is shown in Fig. 2. Fig. 2(a) shows CV results of the Ru/C and Ru_{100-x}Se_x/C catalysts. With Ru/C catalyst in the range 0 - 0.2 V, an anodic peak was attributed to hydrogen desorption from Ru surface.^{40,41} In the region 0.2 - 0.8 V, an increasing anodic current was detected due to the ruthenium surface oxidation and adsorption of water related species, such as the hydroxyl group.^{42,43} The cathodic peak around 0.2 V was caused by reduction of oxidized Ru surface and adsorption of hydrogen on Ru surface.⁴⁴⁻⁴⁶ Increasing Se amount in the catalysts, however, the hydrogen adsorption peak is significantly suppressed, indicating that Ru surface was modified by Se. Furthermore, increasing Se amount, Ru oxidation peaks were significantly suppressed. It was reported that Se stabilized Ru surface against oxidation.⁴⁷ Following the CV studies, we conducted ORR measurements (Fig. 2(b)). For a comparison, Pt/C (E-tek, 60 wt %) is also measured. Current densities at 0.7 V were -1.26, -1.47, -1.55, -1.74, -1.87, -0.95 and -2.23 mA cm⁻² for the Ru/C, Ru₉₅Se₅/C, Ru₉₀Se₁₀/C, Ru₈₅Se₁₅/C, Ru₈₀Se₂₀/C, Ru₇₅Se₂₅/C, and Pt/C. In the Ru based catalysts, the Ru₈₀Se₂₀/C catalyst showed the high-

Table 1. Summary of physical and electrochemical properties of the Ru/C, Ru₉₅Se₅/C, Ru₉₀Se₁₀/C, Ru₈₅Se₁₅/C, Ru₈₀Se₂₀/C, and Ru₇₅Se₂₅/C catalysts

	Physical characterization						Electrochemical characterization		
	XRD		EDS		XPS		ORR		
	(110) Peak (°)	Particle size (nm)	Ru:Se (atom %)	Ru metal	Ru oxide (RuO ₂)	Se	Se oxide (SeO ₂)	Current density at 0.7 V (mA cm ⁻²)	Mass activity (mA g ⁻¹ _{Ru})
Ru/C	69.40	4.9	-	38.0%	62.0 %	-	-	-1.26	-1102.50
Ru ₉₅ Se ₅ /C	69.40	5.1	95.1:4.9	41.0%	59.0%	62.5%	37.5%	-1.47	-1353.95
Ru ₉₀ Se ₁₀ /C	69.42	3.9	89.5:10.5	50.7%	49.3%	63.0%	37.0%	-1.55	-1506.94
Ru ₈₅ Se ₁₅ /C	69.45	3.6	84.0:16.0	56.4%	43.6%	61.4%	38.6%	-1.74	-1797.17
Ru ₈₀ Se ₂₀ /C	69.50	4.1	82.1:17.9	60.6%	39.4%	61.0%	39.0%	-1.87	-2045.31
Ru ₇₅ Se ₂₅ /C	69.50	4.6	76.6:23.4	57.0%	43.0%	63.1%	36.9%	-0.95	-1108.33

**Figure 2.** Electrochemical characterization; Cyclic voltammetry results (a) and ORR results (b) for the Ru/C, Ru₉₅Se₅/C, Ru₉₀Se₁₀/C, Ru₈₅Se₁₅/C, Ru₈₀Se₂₀/C, and Ru₇₅Se₂₅/C catalysts. Tafel plots for the ORR of Ru/C, Ru₉₀Se₁₀/C, and Ru₈₀Se₂₀/C catalysts (c). Methanol tolerance results for the Ru₈₀Se₂₀/C catalyst (d).

est ORR activity which was 84% of the activity of the Pt/C. Activity of the Ru₈₀Se₂₀/C catalyst was higher by 33% than that of the Ru/C. The mass activities were calculated from the current densities. The mass activity of the Ru₈₀Se₂₀/C (-2045.31 mA g⁻¹_{Ru}) showed also the highest activity in the RuSe catalysts. The mass activity of Ru₈₀Se₂₀/C was almost twice as large as that of the Ru/C. The above observations, optimum concentration of RuSe composition was the Ru₈₀Se₂₀/C which is similar with a previous study. Bron *et al.* suggested Ru₈₅Se₁₅ composition as the optimum concentration.⁴⁸ This difference is caused

by difference surface features such as amounts of Ru metal and Ru oxide originated from synthesis process. Se modified Ru catalysts showed the improved ORR activity which has been related to chemical stabilization of metallic Ru surface against oxidation.⁴⁹ Babu *et al.* reported that Se on the Ru surface existed as metallic form due to charge transfer from Ru to Se.⁵⁰ This charge transfer prevents the oxidation of Ru surface. In Fig. 2(c), the kinetic currents are calculated using the Koutecky-Levich (K-L) equation and Tafel plots. The RDE data are analyzed using the K-L equation:

$$\frac{1}{j} = \frac{1}{j_k} + \frac{1}{j_D} = \frac{1}{j_k} + \frac{1}{B\omega^{1/2}} \quad (1)$$

Where j is the measured current density, j_k is the kinetic current density, j_D is the diffusion-limited current density, ω is the rotation rate of the electrode and B is the Levich constant. The value of the B can be obtained from the slope of the K-L plot. The calculated kinetic currents j_k of Ru/C, Ru₉₀Se₁₀/C and Ru₈₀Se₂₀/C are displayed in semi-logarithmic plots versus the potential E . The corrected j_k of three catalysts are compared at 0.7 V. The kinetic current densities at 0.7 V were 1.34, 1.47 and 1.80 mA cm⁻² for the Ru/C, Ru₉₀Se₁₀/C and Ru₈₀Se₂₀/C.

The Ru₈₀Se₂₀/C catalyst showed the highest kinetic activity. As shown in the Tafel plot, Se modification of the Ru surface leads to increasing the catalytic activity of the Ru catalyst. The Ru₈₀Se₂₀/C catalyst showed significantly high methanol tolerant property compared to the Pt/C (Fig. 2(d)). The current density under methanol environment of Ru₈₀Se₂₀/C catalyst was ~1.82 mA cm⁻², which is 97.3% performance of the activity without methanol. It is the reason that Ru catalyst has almost no methanol oxidation property. The high methanol property make Ru₈₀Se₂₀/C a powerful candidate as a cathode material of DMFCs. A summary of the electrochemical analysis results is tabulated in Table 1.

Fig. 3 exhibits the XPS results of Ru 3d core level for Ru₉₅Se₅/C (Fig. 3(a)) and Ru₈₀Se₂₀/C (Fig. 3(b)). The results of all catalysts for Ru 3d core level are summarized in Table 1. The prepared catalysts were supported by Vulcan XC72R carbon material which shows the large C 1s peak in 284.5 eV. The metallic Ru doublet with 3d_{5/2} and 3d_{3/2} components shows peaks at 280.1 eV and 284.3 eV, respectively.⁵¹ From peak deconvolution, the Ru surface was composed of a metallic Ru and an oxide form. The RuO₂ doublet with 3d_{5/2} and 3d_{3/2} components exhibit peaks at 281.3 eV and 285.5 eV, respectively.^{52,53} The ratios of the metallic Ru to RuO₂ were calculated from the area of the 3d_{5/2} peaks. The Ru/C catalyst was composed of 38% metallic Ru and 62% RuO₂. With increased Se amounts, amounts of metallic Ru on the catalysts surfaces were increased up to 60.6% on the Ru₈₀Se₂₀/C surface. In the case of Ru₇₅Se₂₅/C catalysts, similar surface composition with Ru₈₀Se₂₀/C was observed. It has good agreement with previous study. As mentioned above, Se modification on Ru surface makes Ru surface metallic. Lewera *et al.* suggested that the oxygen in the Ru surface is strongly bonded to Ru, and Se is weakening the Ru-O bond.⁵⁴ In Fig. 3(c), the XPS result of Se 3d core level for Ru₈₀Se₂₀/C is exhibited. The results of all catalysts for Se 3d core level are summarized in Table 1. The binding energy peak for Se 3d_{3/2} peak appear at 55.2 eV. The Se 3d_{5/2} peak for oxidized form appears at about 58.5 - 59.0 eV.^{52,53} The Ru₈₀Se₂₀/C catalyst was composed of 61.0% elemental Se and 39.0% oxidized Se. Other catalysts show similar results to Ru₈₀Se₂₀/C. All catalysts appeared the large amount of oxidized Se. In a previous study, Zhu *et al.* reported that elemental Se powder were synthesized by polyol method in similar conditions.⁵⁵ It means that reduction of the Se was affected by the Ru species. The oxidized Se on the RuSe catalysts should be affected by the charge transfer from Ru to Se on Se modified Ru surface.

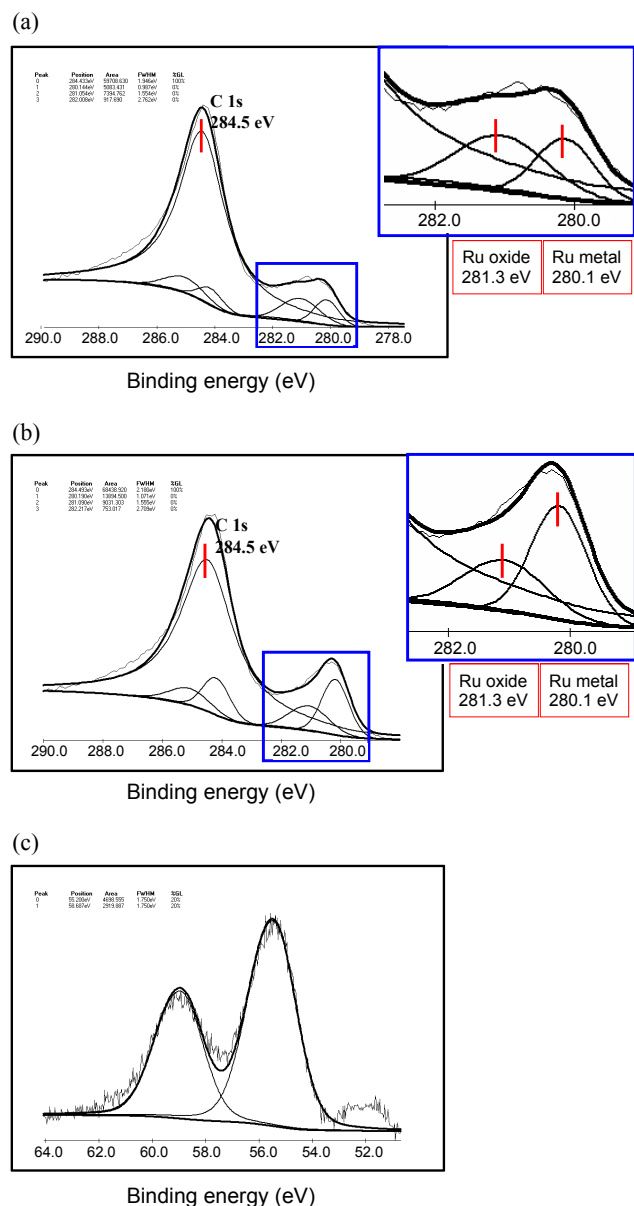


Figure 3. The XPS spectra of the Ru₉₅Se₅/C and Ru₈₀Se₂₀/C: Ru 3d regions for the Ru₉₅Se₅/C (a) and the Ru₈₀Se₂₀/C (b) catalysts and Se 3d region for the Ru₈₀Se₂₀/C (c).

Fig. 4 shows the single cell performance of Ru₈₀Se₂₀/C catalyst. The commercial Pt/C was prepared for comparison. MEA1 was composed of PtRu/C (anode) and Pt/C (cathode) and MEA2 was composed of PtRu/C (anode) and Ru₈₀Se₂₀/C (cathode). The open circuit voltages (OCV) of MEA1 and MEA2 were 0.62 V and 0.70 V, respectively. The MEA2 showed improved OCV due to outstanding methanol tolerant property of Ru₈₀Se₂₀/C which is exhibited in electrochemical study. As expected, MEA1 showed much higher max power density, 73.5 mW cm⁻² than MEA2. Max power density of MEA2 was 39.5 mW cm⁻². The Ru₈₀Se₂₀/C which is non-Pt cathode material showed 53.6% max power density and the improved OCV when comparing with Pt/C. This is suitable for cathode material to substitute Pt but the improved ORR activity of RuSe catalysts is essential.

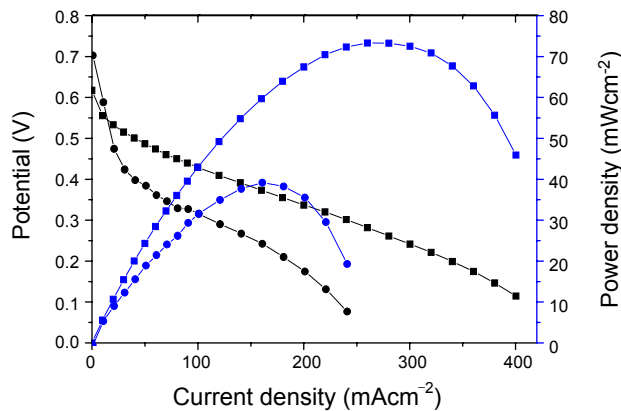


Figure 4. The single cell performances for MEA1 (■, anode : PtRu/C, cathode : Pt/C) and MEA2 (●, anode : PtRu/C, cathode : Ru₈₀Se₂₀/C) in DMFC.

Conclusions

The Se modified Ru catalysts were synthesized via a polyol method. By adding Se component, amounts of metallic Ru surface were increased and improvement of ORR activity was achieved. Optimum concentration of RuSe composition was the Ru₈₀Se₂₀/C which is almost twice as higher than Ru/C in mass activity. Furthermore, the Ru₈₀Se₂₀/C showed prominent methanol tolerant property. Electrochemical characterization and single cell measurement showed that the Ru₈₀Se₂₀/C is suitable for cathode material of DMFCs.

Acknowledgments. This work was supported by the Korea Science & Engineering Foundation (KOSEF) grant (WCU program, 31-2008-000-10055-0) funded by the Ministry of Education and Science & Technology (MEST) and the National Research Foundation of Korea(NRF) grant funded by the MEST (No. 2009-0092783).

References

1. Jeon, M. K.; Lee, K. R.; Oh, K. S.; Hong, D. S.; Won, J. Y.; Li, S.; Woo, S. I. *J. Power Sources* **2006**, *158*, 1344.
2. Choi, W. C.; Kim, J. D.; Woo, S. I. *Catal. Today* **2002**, *74*, 235.
3. Jeon, M. K.; Won, J. Y.; Woo, S. I. *Electrochim. Solid-State Lett.* **2007**, *10*, B25.
4. Choi, W. C.; Kim, J. D.; Woo, S. I. *J. Power Sources* **2001**, *96*, 411.
5. Antolini, E. *Appl. Catal. B: Environ.* **2007**, *74*, 337.
6. Lee, K. R.; Jeon, M. K.; Woo, S. I. *Appl. Catal. B-Environ.* **2009**, *91*, 428.
7. Jeon, M. K.; Lee, K. R.; Jeon, H. J.; Woo, S. I. *J. Appl. Electrochem.* **2009**, *39*, 1503.
8. Travitsky, N.; Ripenbein, T.; Golodnitsky, D.; Rosenberg, Y.; Burshtein, L.; Pele, E. *J. Power Sources* **2006**, *161*, 782.
9. Whitacre, J. F.; Valdez, T. I.; Narayanan, S. R. *Electrochim. Acta* **2008**, *53*, 3680.
10. Jeon, M. K.; Zhang, Y.; McGinn, P. J. *Electrochim. Acta* **2010**, *55*, 5318.
11. Schulenburg, H.; Müller, E.; Khelashvili, G.; Roser, T.; Bönnemann, H.; Wokaun, A.; Scherer, G. G. *J. Phys. Chem. C* **2009**, *113*, 4069.
12. Antolini, E.; Salgado, J. R. C.; Santos, L. G. R. A.; Garcia, G.; Ticianelli, E. A.; Pastor, E.; Gonzalez, E. R. *J. Appl. Electrochem.* **2006**, *36*, 355.
13. Jeon, M. K.; Liu, J. H.; Lee, K. R.; Lee, J. W.; McGinn, P. J.; Woo, S. I. *Fuel Cells* **2010**, *10*, 93.
14. Liu, J. H.; Jeon, M. K.; Woo, S. I. *Appl. Surf. Sci.* **2006**, *252*, 2580.
15. Choi, W. C.; Woo, S. I.; Jeon, M. K.; Sohn, J. M.; Kim, M. R.; Jeon, H. J. *Adv. Mater.* **2005**, *17*, 446.
16. Jeon, M. K.; Lee, K. R.; Lee, W. S.; Daimon, H.; Nakahara, A.; Woo, S. I. *J. Power Sources* **2008**, *185*, 927.
17. Gupta, G.; Slanac, D. A.; Kumar, P.; Camacho, J. D. W.; Kim, J.; Ryoo, R.; Stevenson, K. J.; Johnston, K. P. *J. Phys. Chem. C* **2010**, *114*, 10796.
18. Gasteiger, H. A.; Kocha, S. S.; Sompalli, B.; Wagner, F. T. *Appl. Catal. B* **2005**, *56*, 9.
19. Srivastava, R.; Mani, P.; Hahn, N.; Strasser, P. *Angew. Chem. Int. Ed.* **2007**, *46*, 8988.
20. Antolini, E.; Lopes, T.; Gonzalez, E. R. *J. Alloys. Comp.* **2008**, *461*, 253.
21. DeLuca, N. W.; Elabd, Y. A. *J. Polym. Sci. Polym. Phys.* **2006**, *44*, 2201.
22. Suo, Y.; Zhuang, L.; Lu, J. *Angew. Chem. Int. Ed.* **2007**, *46*, 2862.
23. Shao, M. H.; Sasaki, K.; Adzic, R. R. *J. Am. Chem. Soc.* **2006**, *128*, 3526.
24. Sarker, A.; Murugan, A. V.; Manthiram, A. *J. Phys. Chem. C* **2008**, *112*, 12037.
25. Widelov, A.; Larsson, R. *Electrochim. Acta* **1992**, *37*, 187.
26. Bashyam, R.; Zelenay, P. *Nature* **2006**, *443*, 63.
27. Babu, P. K.; Lewera, A.; Chung, J. H.; Hunger, R.; Jaegermann, W.; Vante, N. A.; Wiechowski, A.; Oldfield, E. *J. Am. Chem. Soc.* **2007**, *129*, 15140.
28. Lee, J. W.; Popov, B. N. *Solid State Electrochem.* **2007**, *11*, 1355.
29. Lee, K. R.; Lee, K. U.; Lee, J. W.; Ahn, B. T.; Woo, S. I. *Electrochim. Commun.* **2010**, in press.
30. Liu, G. C.; Dahn, J. R. *Appl. Catal. A: General* **2008**, *347*, 43.
31. Matter, P. H.; Zhang, L.; Ozkan, U. S. *J. Catal.* **2006**, *239*, 83.
32. Vante, N. A.; Jaegermann, W.; Tributsch, H.; Honle, W.; Yvon, K. *J. Am. Chem. Soc.* **1897**, *109*, 3251.
33. Vante, N. A.; Tributsch, H.; Feria, O. S. *Electrochim. Acta* **1995**, *40*, 567.
34. Fievet, F.; Lagier, J. P.; Blin, L. B.; Beaudoin, B.; Figlarz, M. *Solid State Ionics* **1989**, *32/33*, 198.
35. Yan, S.; Sun, G.; Tian, J.; Jiang, L.; Qi, J.; Xin, Q. *Electrochim. Acta* **2006**, *52*, 1692.
36. Schmidt, T. J.; Gasteiger, H. A.; Stäb, G. D.; Urban, P. M.; Kolb, D. M.; Behm, R. J. *J. Electrochem. Soc.* **1998**, *145*, 2354.
37. Li, W.; Zhou, W.; Li, H.; Zhou, Z.; Zhou, B.; Sun, G.; Xin, Q. *Electrochim. Acta* **2004**, *49*, 1045.
38. Serov, A. A.; Min, M.; Chai, G.; Han, S.; Kang, S.; Kwak, C. J. *Power Sources* **2008**, *175*, 175.
39. He, C. Z.; Kunz, H. R.; Fenton, J. M. *J. Electrochim. Soc.* **1997**, *144*, 970.
40. Cao, D.; Wiechowski, A.; Inukai, J.; Vante, N. A. *J. Electrochimical Soc.* **2006**, *153*(5), A869.
41. Nagabushana, K. S.; Dinjus, E.; Bönnemann, H.; Zaikovskii, V.; Hartnig, C.; Zehl, G.; Dorbandt, I.; Fiechter, S.; Bogdanoff, P. J. *Appl. Electrochem.* **2007**, *37*, 1515.
42. Jordanov, S. H.; Kozlowska, H. A.; Vukovic, M.; Conway, B. E. *J. Phys. Chem.* **1977**, *81*, 2271.
43. Colmenares, L.; Jusys, Z.; Behm, R. J. *J. Phys. Chem. C* **2007**, *111*, 1273.
44. Michell, D.; Rand, D. A. J.; Woods, R. *J. Electroanal. Chem. Interfacial Electrochem.* **1978**, *89*, 11.
45. Kinoshita, K.; Ross, P. N. *J. Electroanal. Chem. Interfacial Electrochem.* **1977**, *78*, 313.
46. Pinheiro, A. L. N.; Zei, M. S.; Ertl, G. *Phys. Chem. Chem. Phys.* **2005**, *7*, 1300.
47. Dassenoy, F.; Vogel, W.; Vante, N. A. *J. Phys. Chem. B* **2002**, *106*, 12152.
48. Bron, M.; Bogdanoff, P.; Fiechter, S.; Dorbandt, I.; Hilgendorff,

- M.; Schulenburg, G.; Tributsch, H. *J. Electroanal. Chem.* **2001**, *500*, 510.
49. Colmenares, L.; Jusys, Z.; Behm, R. J. *Langmuir* **2006**, *22*, 10437.
50. Babu, P. K.; Lewera, A.; Chung, J. H.; Hunger, R.; Jaegermann, W.; Vante, N. A.; Wiechowski, A.; Oldfield, E. *J. Am. Chem. Soc.* **2007**, *129*, 15140.
51. Wagner, C. D.; Naumkin, A. V.; Vass, A. K.; Allison, J. W.; Powell, C. J.; Rumble, J. R., Jr. NIST standard Reference Database 20, Version 3.4.
52. Vericat, C.; Wakisaka, M.; Haasch, R.; Bagus, P. S.; Wiechowski, A. *J. Solid State Electorhcem.* **2004**, *8*, 794.
53. Rochefort, D.; Dabo, P.; Guay, D.; Sherwood, P. M. A. *Electrochim. Acta* **2003**, *48*, 4245.
54. Lewera, A.; Inukai, J.; Zhou, W. P.; Cao, K.; Duong, H. T.; Vante, N. A.; Wiechowski, A. *Electrochimica Acta* **2007**, *52*, 5759.
55. Zhu, Y. J.; Hu, X. L. *Mater. Lett.* **2004**, *58*, 1234.